Downregulation of Connexin 43 Expression by High Glucose Induces Senescence in Glomerular Mesangial Cells

Xiaojie Zhang, Xiangmei Chen, Di Wu, Weiping Liu, Jianzhong Wang, Zhe Feng, Guangyan Cai, Bo Fu, Quan Hong, and Jing Du

Department of Nephrology, Kidney Center and Key Lab of the People's Liberation Army, General Hospital of People's Liberation Army, Beijing, People's Republic of China

Connexin 43 (Cx43) plays an important role in cell differentiation and growth control, but whether it can be regulated by high glucose and whether it can mediate in glomerular mesangial cells (GMC) the phenotype alterations that are induced by high glucose still remain to be explored. In this study, RNA interference and gene transfer techniques were used to knock down and overexpress Cx43 gene in rat GMC to determine the contribution of Cx43 to GMC senescence that was induced by high glucose. The results show that high glucose (30 mM) not only downregulated Cx43 mRNA and protein expression ($P < 0.05$) but also increased the percentage of senescence-associated β-galactosidase (SA-β-gal) stained cells and expression of $p21^{cip1}$ and $p27^{kip1}$ ($P < 0.05$), indicating that high glucose promoted rat GMC senescence. Knocking down Cx43 gene expression significantly increased the percentage of SA-β-gal stained cells and $p27^{kip1}$ and $p21^{cip1}$ expression in GMC ($P < 0.05$), whereas overexpression of Cx43 significantly decreased the percentage of SA-β-gal stained cells ($P < 0.05$). These results demonstrate for the first time that downregulation of Cx43 expression by high glucose promotes the senescence of GMC, which may be involved in the pathogenesis of diabetic nephropathy.

J Am Soc Nephrol 17: 1532–1542, 2006. doi: 10.1681/ASN.2005070776

Hypertrophy of glomerular mesangial cells (GMC) is one of the earliest morphologic alterations in the kidney after the onset of diabetes. Previous studies (1–3) have shown that cultured GMC that are exposed to high glucose arrest in the G1 phase of the cell cycle, with an increased expression of the cyclin-dependent kinase (CDK) inhibitors $p21^{cip1}$ and $p27^{kip1}$, which are markers of cell senescence (4,5).

Blazer *et al.* (6) reported that hyperglycemia induced premature replicative senescence in human skin fibroblasts. Morocutti *et al.* (7) demonstrated that there was retardation of the cell replication rate, which was tightly coupled to larger cell volume in skin fibroblasts from patients with diabetic nephropathy. These results showed that high glucose was associated with the fibroblast aging process, although the mechanisms remained unclear.

There is some evidence (8–11) that connexin 43 (Cx43) expression and intercellular communication in retinal endothelial cells and aortic smooth muscle cells are reduced under conditions of hyperglycemia, contributing to the development of the microangiopathy and macroangiopathy that are associated with diabetes. However, the relationship between Cx43 and cell senescence is yet unclear. Our hypothesis here is that high glucose may promote GMC senescence through downregulation of Cx43 expression and function.

This study was designed to investigate the effects of high glucose on senescence of GMC, expression of Cx43, and changes of gap junctional intercellular communication (GJIC). In addition, we aimed to determine the relationship between Cx43 and GMC senescence under high glucose conditions. Our results indicate that reduced Cx43 expression under high glucose accelerates the progression of mesangial cell senescence, a mechanism that is associated with mesangial cell hypertrophy in diabetic nephropathy.

Materials and Methods

Materials

FBS and DMEM were supplied by Life Technologies BRL (Gaithersburg, MD). The retrovirus packaging cell line PT-67 and retroviral vector pLNCX2 were obtained from Clontech Laboratories (Palo Alto, CA). Penicillin, streptomycin, and TRIzol reagent were from Invitrogen (Carlsbad, CA). Polybrene, leupeptin, aprotinin, antipain, phenylmethylsulfonyl fluoride, and Ac-DEVD-CHO were procured from Sigma (St. Louis, MO). The NIH 3T3 cell line was obtained from the cell bank of the Chinese Academy of Sciences. SuperFect was purchased from Qiagen (Valencia, CA). Antibodies were procured from Sigma (Cx43 and hemagglutinin [HA]) and Santa Cruz Biotechnology (Santa Cruz, CA; $p27^{kip}$ and $p21^{cip}$).

Cell Culture

Primary rat GMC were obtained from male Wistar rats (3 mo of age). The cells were grown in low-glucose DMEM (5.5 mM D-glucose) that was supplemented with 15% FBS, 100 units/ml penicillin, and 100 μg/ml streptomycin at 37°C (12). Cells from passages 3 to 5 were used in our study. For determination of the effects of high glucose on Cx43

Received July 27, 2005. Accepted March 14, 2006.

Published online ahead of print. Publication date available at www.jasn.org.

Address correspondence to: Dr. Xiangmei Chen, Department of Nephrology, Kidney Center and Key Lab of PLA, General Hospital of PLA, 28 Fuxing Road, Beijing 100853, People's Republic of China. Phone: +86-10-66935462; Fax: +86-10-68130297; E-mail: xmchen@public.bta.net.cn

ISSN: 1046-6673/1706-1532

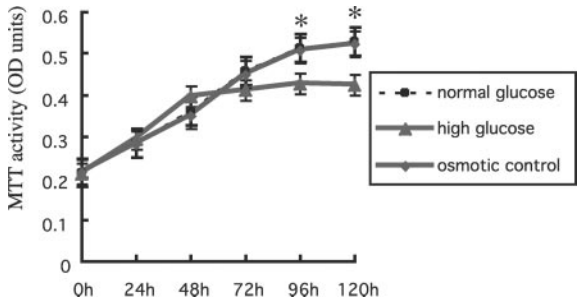

Figure 1. Effect of high glucose on proliferation of glomerular mesangial cells (GMC). Cells were grown for specified periods of time, and cell number was determined using 3-(4,5-dimethylthiazol-2-yl)-2,5-(diphenyltetrazolium bromide) (MTT) conversion, measured spectrophotometrically (optical density [OD]). After 24 or 48 h of incubation, cellular proliferation of the high-glucose group was slightly higher than that of the normal-glucose group or the osmotic control group. However, after 72 h, cellular proliferation was permanently inhibited in the high-glucose group in which the OD value was significantly lower than those of the other two groups. Values are means ± SD ($n = 6$); comparison among groups was conducted with ANOVA. *$P < 0.05$ *versus* control.

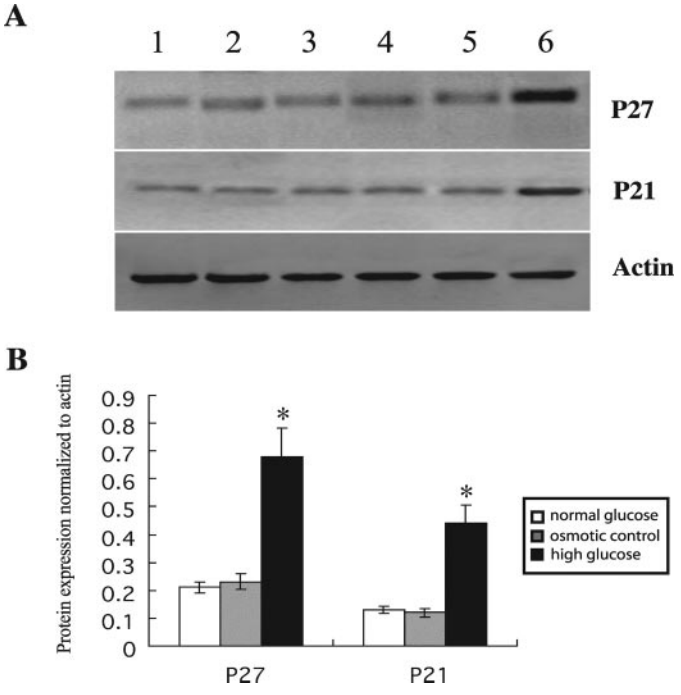

Figure 2. Effect of high glucose on $p27^{kip1}$ and $p21^{cip1}$ expression of GMC. Cells were grown for 48 h under various glucose conditions and then were harvested for Western blot analysis. (A) Western blot of $p27^{kip1}$ and $p21^{cip1}$. Lanes 1 through 3, GMC in the normal-glucose group, osmotic control group, and high-glucose group, respectively, after 24 h of incubation; lanes 4 through 6, GMC of the normal-glucose group, osmotic control group, and high-glucose group, respectively, after 48 h of incubation. (B) $p27^{kip1}$ and $p21^{cip1}$ expression. Data are expressed as relative percentages *versus* actin, and groups were compared using ANOVA. *$P < 0.05$ *versus* normal-glucose group ($n = 6$).

expression and GJIC activity, GMC were grown in normal (5.5 mM) or high (30 mM) D-glucose medium for 48 or 96 h. As an osmotic control, GMC were grown in normal-glucose medium that contained 24.5 mM mannitol. The PT-67 retroviral packaging cells and NIH3T3 cells were cultured in DMEM with 10% FBS, 10 mM HEPES, 2 mM L-glutamine, 1 mM MEM sodium pyruvate, 100 units/ml penicillin, and 100 μg/ml streptomycin.

Cells Proliferation Capacity Analyses

Cells were seeded into 96-well plates (2×10^3 cells/well). After incubation for 24, 48, 72, and 96 h, respectively, 3-(4,5-dimethylthiazol-2-yl)-2,5-(diphenyltetrazolium bromide) (MTT) (2 mg/ml, 20 μl) was added into each well and incubated for 4 h. DMSO (100 μl) subsequently was added to each well to dissolve the formazan crystals, and the absorption at 570 nm was measured.

Total Protein/Cell Number Ratio

Because the total protein/cell number ratio is a well-established measurement of cellular hypertrophy, this parameter was used to determine whether the alteration of cell growth was accompanied by cell hypertrophy (13). GMC were cultured for 1 to 4 d in low- or high-glucose medium, and at the end of the treatment period, cells were trypsinized and washed twice with ice-cold PBS and counted in a hemocytometer chamber. The cells then were lysed to measure the total protein content by the Bradford method. The total protein/cell number ratio expressed as $\mu g/10^5$ cells was used as a hypertrophy index.

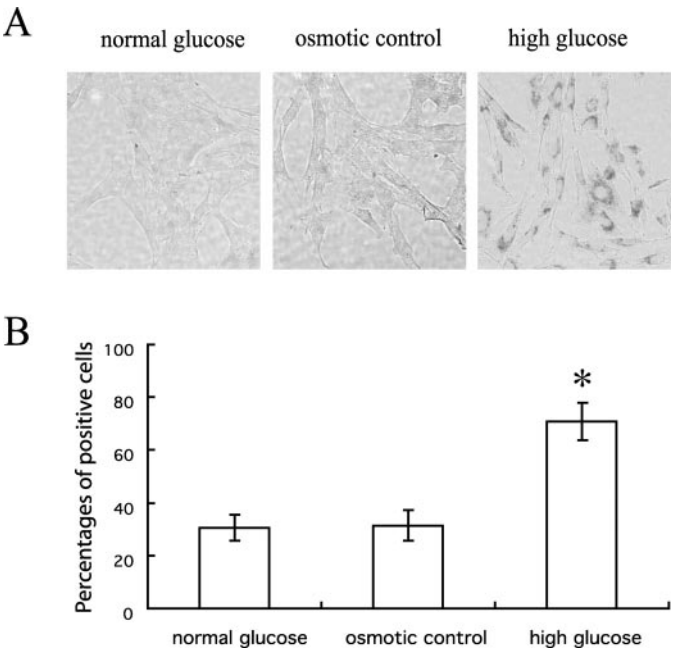

Figure 3. Effect of high glucose on senescence-associated β-galactosidase (SA-β-gal) staining of GMC. (A) GMC grown in normal glucose, osmotic control conditions, and high glucose for 96 h of incubation were stained for SA-β-gal, which shows blue precipitation in the cytoplasm in senescent cells. (B) The percentage of SA-β-gal stained positive cells. For each group, 100 to 200 cells were counted. Comparison among groups was conducted with ANOVA. *$P < 0.05$ *versus* normal-glucose group. Magnification, ×200.

Senescence-Associated β-Galactosidase Staining

After washing in PBS and fixation for 3 to 5 min (room temperature) in 2% formaldehyde/0.2% glutaraldehyde, the cells were incubated overnight at 37°C (without CO_2) with freshly prepared senescence-associated β-galactosidase (SA-β-gal) stain solution (1 mg/ml X-gal, 40 mM citric acid/sodium phosphate [pH 6.0], 5 mM potassium ferrocyanide, 5 mM potassium ferricyanide, 150 mM NaCl, and 2 mM $MgCl_2$). Cells then were rinsed with PBS, and 100 to 200 cells in six microscopic fields were counted to determine the percentages of SA-β-gal stained positive cells.

Cell-Cycle Analysis

Cells (1×10^6; each sample) were treated with 0.25% trypsin, washed twice with cold PBS, and fixed with 70% alcohol in PBS for 12 h at 4°C. The cells then were washed twice with PBS and stained for 30 to 60 min at 4°C in 100 μg/ml propidium iodide solution (with 100 μg/ml RNase). Stained cells were analyzed by flow cytometry (Becton Dickinson, Franklin Lakes, NJ).

Real-Time PCR Assay

Cx43 mRNA expression was measured by real-time PCR with the following primers: Sense 5′-TTC ATG CTG GTG GTG TCC-3′ and antisense 5′-TTG GCA TTC TGG TTG TCG-3′ (expected product of approximately 400 bp). Control glyceraldehyde-3-phosphate dehydrogenase primers were as follows: Sense 5′-TGC ACC ACC AAC TGC TTA GC-3′ and antisense 5′-GGC ATG GAC TGT GGT CAT GAG-3′. Real-time PCR was performed with SYBR green I (1:20,000; Qiagen), with 1 cycle at 95°C for 3 min followed by 40 cycles at 95°C for 45 s, 61°C for 45 s, 72°C for 40 s, and 80°C for 5 s.

Western Blotting

The cells were lysed in RIPA buffer that was composed of 50 mM Tris-Cl (pH 7.6), 5 mM EDTA, 150 mM NaCl, 0.5% NP-40, and 0.5% Triton-X-100 and contained 1 μg/ml leupeptin, aprotinin, and antipain; 1 mM sodium orthovanadate; and 0.5 mM phenylmethylsulfonyl fluoride. Protein concentration was measured by the Bradford assay. A total of 50 μg of total protein was separated by 12% SDS-PAGE and then transferred to a membrane, which was blocked with 5% skim milk, probed with a primary antibody overnight at 4°C, and incubated with an horseradish peroxidase–conjugated secondary antibody. Immunoreactive bands were visualized using enhanced chemiluminescence.

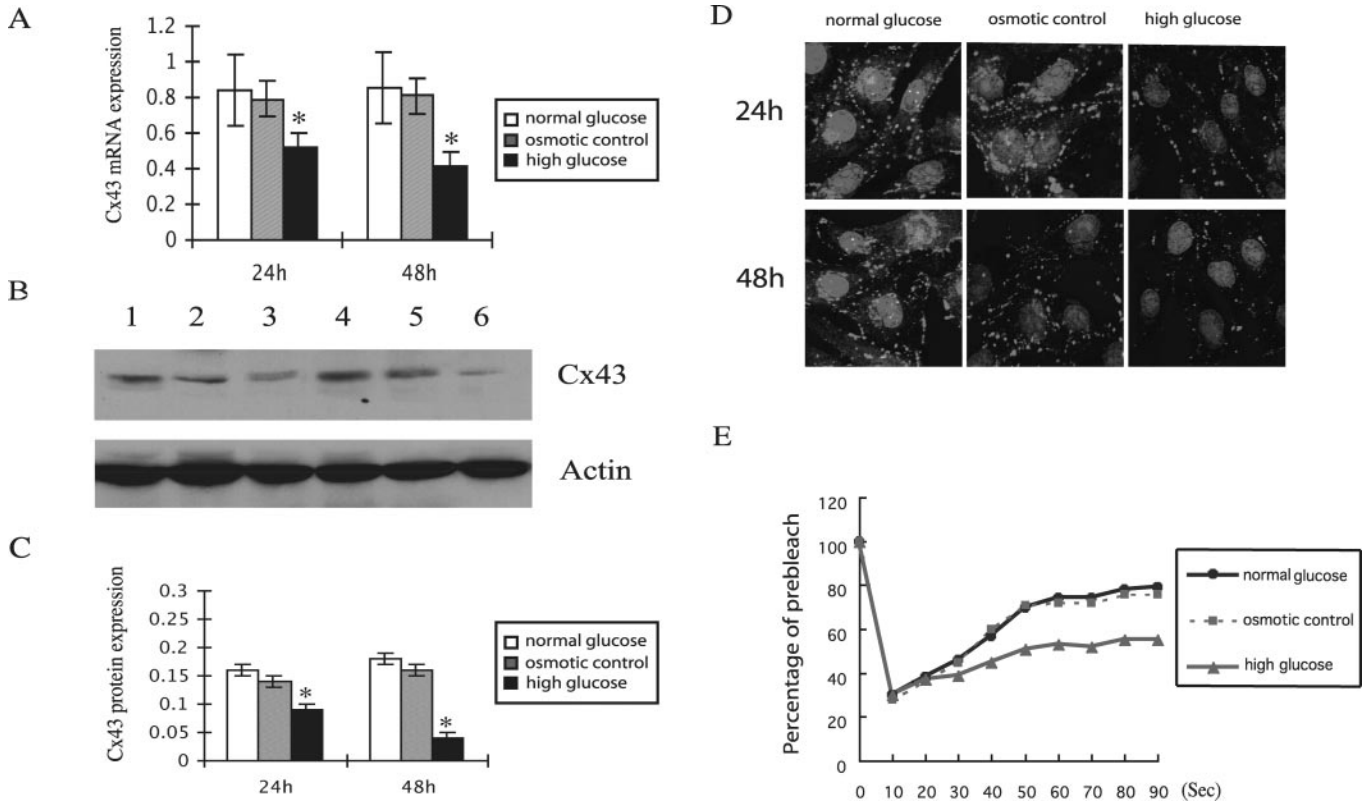

Figure 4. Effect of high glucose on connexin 43 (Cx43) expression and gap junctional intercellular communication (GJIC) function of GMC. (A) Cx43 mRNA expression was detected by real-time PCR. Data are expressed as relative percentages against glyceraldehyde-3-phosphate dehydrogenase (GAPDH). *$P < 0.05$ *versus* normal glucose group ($n = 6$). (B) Western blot of Cx43 proteins. Lanes 1 through 3, GMC of normal-glucose group, osmotic control group, and high-glucose group, respectively, after 24 h of incubation; lanes 4 through 6, GMC of normal-glucose group, osmotic control group, and high-glucose group, respectively, after 48 h of incubation. (C) Graphic presentation of relative Cx43 protein abundances compared with actin. *$P < 0.05$ *versus* normal-glucose group ($n = 6$). (D) Immunofluorescence staining of Cx43 with monoclonal anti-Cx43 antibody. Note the characteristic spotted staining of Cx43 at the cell–cell contact regions. (E) Fluorescence recovery curve (in seconds) after photobleaching detected by fluorescence recovery after photobleaching (FRAP). GMC were cultured under normal-glucose medium, osmotic control, and high-glucose medium for 48 h. The data shown are from one representative experiment from a series of five with similar results. Magnification, ×600.

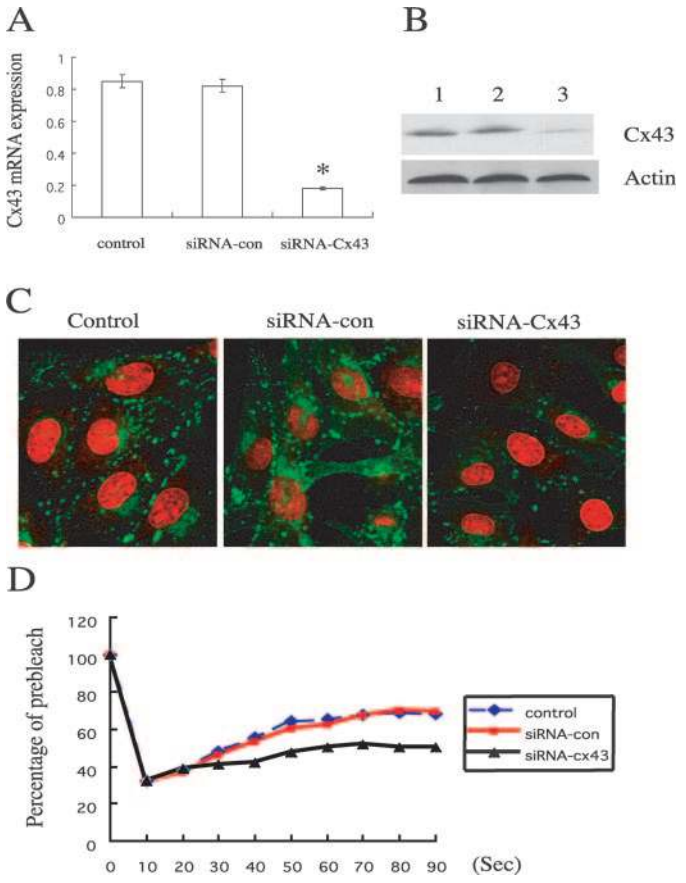

Figure 5. Inhibition of Cx43 expression in GMC by small interference RNA (siRNA). (A) Cx43 mRNA expression detected by real-time PCR. GMC transfected with siRNA-Cx43 had a dramatically lower Cx43 mRNA expression than that of control and GMC transfected with siRNA-con. The graph summarizes combined real-time PCR data from at least six separate experiments in which the expression level of Cx43 mRNA was quantified and normalized to GAPDH. $^*P < 0.05$ *versus* control group. (B) Western blot revealed a significant reduction of total Cx43 protein expression in GMC transfected with siRNA-Cx43 (lane 3) compared with control (lane 1) and GMC transfected with siRNA-con (lane 2). (C) GMC were transfected with siRNA-Cx43 and siRNA-con and then immunostained for Cx43. Note that siRNA-Cx43–expressing cells had a dramatically reduced number of gap junctions. (D) Fluorescence recovery curve detected by FRAP method. GJIC of GMC was inhibited dramatically by siRNA-Cx43 transfection. The data shown are from one representative experiment from a series of five with similar results. Magnification, ×600.

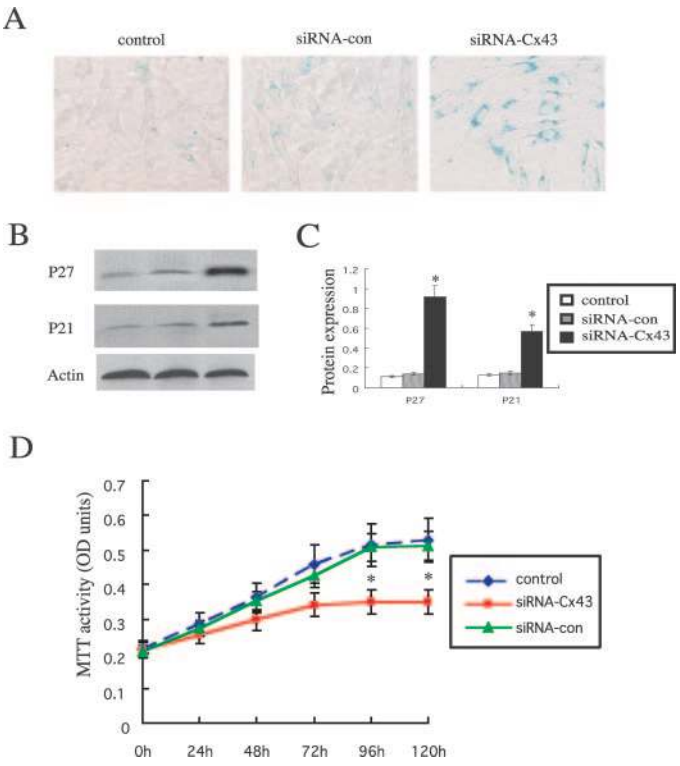

Figure 6. Senescence-related phenotypes in GMC transfected with siRNA. (A) Effect of siRNA inhibition of Cx43 on SA-β-gal staining of GMC. The percentage of SA-β-gal–positive cells after transfection with siRNA-Cx43 was higher than that of control or cells transfected with siRNA-con. (B) $p27^{kip1}$ and $p21^{cip1}$ protein expression detected by Western blot. Note that both $p27^{kip1}$ and $p21^{cip1}$ expression was higher in GMC transfected with siRNA-Cx43 (lane 3) than in GMC of control group (lane 1) and in GMC transfected with siRNA-con (lane 2). (C) Relative $p27^{kip1}$ and $p21^{cip1}$ protein abundances normalized to actin. The results showed that the expression levels of $p27^{kip1}$ and $p21^{cip1}$ proteins in cells transfected with siRNA-Cx43 were significantly elevated compared with those in the control group or siRNA-con group. $^*P < 0.05$ *versus* control group ($n = 6$). (D) Proliferation of GMC transfected with siRNA-Cx43 was lower than that of control or cells that wee transfected with siRNA-con. $^*P < 0.05$ *versus* control group ($n = 6$). Magnification, ×200.

Immunofluorescence Detection

To study the distribution and relative amounts of Cx43, we performed immunofluorescent staining for Cx43 in GMC using a routine procedure. Briefly, rat GMC were seeded on sterile glass coverslips and grown to confluence, fixed in 4% paraformaldehyde for 15 min at 4°C, washed in PBS, then permeabilized with 1% Triton X-100. After blocking nonspecific antibody binding with 1% BSA for 15 min, the cells were incubated overnight at 4°C in a moist chamber with a monoclonal mouse anti-rat Cx43 antibody diluted at 1:400 in PBS that contained 1% BSA. After washing with PBS three times, the cells were incubated for 1 h with FITC-conjugated anti-mouse IgG (Sigma) diluted at 1:100 in PBS that contained 1% BSA. After three PBS washes, the cells were counterstained with propidium iodide and photographed using a confocal microscope (Radiance 2000; Bio-Rad Laboratories) equipped with LSM510 software.

Fluorescence Recovery after Photobleaching

The degree of intercellular communication between neighboring cultured GMC was determined by fluorescence recovery after photobleaching (FRAP) (14), which has been a powerful tool to measure cell-to-cell diffusion of a fluorescent dye under a laser scanning microscope (Radiance 2000, Bio-Rad Laboratories). Briefly, the cells were loaded for 20 min at room temperature with the membrane-permeant dye 6-carboxyfluorescein diacetate (50 μM; Molecular Probes, Eugene,

Table 1. Silencing Cx43 expression triggered hypertrophy in GMC[a]

	Control	siRNA-con	siRNA-Cx43
Protein/cell number ratio	24.45 ± 2.61	24.56 ± 3.86	31.64 ± 5.63[b]

[a]Glomerular mesangial cells (GMC) were transfected with small interference RNA–connexin 43 (siRNA-Cx43) and siRNA-con. Total protein content was determined by Bradford assays, and cells were counted manually to determine the total protein/cell number ratio expressed as $\mu g/10^5$ cells. Values are means ± SD ($n = 6$); comparison among groups was conducted by ANOVA.
[b]$P < 0.05$ *versus* control group.

Table 2. Silencing Cx43 expression blocks the cell-cycle progression of GMC[a]

	Control	siRNA-con	siRNA-Cx43
G1 phase	60.18 ± 6.08	56.34 ± 5.17	74.6 ± 8.14[b]
S phase	37.94 ± 4.32	39.12 ± 4.68	25.07 ± 2.16[b]

[a]GMC were transfected with siRNA-Cx43 and siRNA-con and stained with propidium iodide to label nuclear DNA; DNA content was analyzed by flow cytometry. Values are means ± SD ($n = 6$); comparison among groups was conducted by ANOVA.
[b]$P < 0.05$ *versus* control group.

OR). Then, a region of the cell is bleached briefly using a 488-nm argon laser spot at 90% of full power for 10 s. Consequently, the cells inside the region of illumination irreversibly lose their fluorescence, a phenomenon that is known as photobleaching. Because cells can communicate with neighboring cells through gap junctions, the unbleached dye from adjacent cells can move into the bleached region, and fluorescence inside the bleached zone increases and eventually reaches an equilibrium state. Recovery of fluorescence was quantified at 5-s intervals for 12 min to derive recovery curves. We derived the recovery ratio to prephotobleaching and the diffusion speed of various experimental groups of GMC using these curves and were able to estimate their GJIC functional status.

Small Interference RNA Experiments

The small interference RNA (siRNA) was designed to target the following sequence of rat Cx43 sequence (GenBank, X06656): AAT GAA GCA GAT TGA AAT CAA. The corresponding primers were used to produce siRNA-Cx43 using the Silencer siRNA construction kit (Ambion, Inc., Austin, TX): Sense 5′-AAT TGA TTT CAA TCT GCT TCA CCT GTC TC-3′ and antisense 5′-AAT GAA GCA GAT TGA AAT CAA CCT GTC TC-3′. GMC were transfected with 0.15 μg of siRNA-Cx43 for 48 h, then Cx43 mRNA and protein expression were studied by real-time PCR and Western blotting, respectively. To confirm the specificity of siRNA-Cx43, we used a nonsense sequence siRNA-con as a control.

Construction of Retroviral Vectors and Transfection of GMC

cDNA encoding full-length Cx43 with an HA tag was subcloned into the Bgl II/SalI sites of retroviral vector pLNCX2-neo (Clontech Co., Mountain View, CA) to create pLNCX2-Cx43. The packaging cell line PT-67 was transfected by Lipofectamine 2000 with 15 μg of pLNCX2-Cx43 or pLNCX2-neo. The retroviruses were collected from the culture medium 48 h after transfection, passed through a 0.45-μm filter, and spun at 50,000 × *g* for 1.5 h. The retroviruses were resuspended overnight in TNE buffer with 0.l times the original volume at 4°C and stored at −80°C. NIH3T3 cells were used to determine viral titers. Briefly, the cells were infected with the virus for 24 h, selected with 300 μg/ml G418 for 1 wk, fixed with 4% formaldehyde, and stained with Giemsa.

The efficiency of pLNCX2-Cx43 infection of GMC was demonstrated by Western blotting against the HA tag and immunofluorescent double staining with Cx43 and HA antibodies. The latter was done as follows: GMC were fixed in 4% paraformaldehyde, permeabilized, and blocked, and the cells were incubated overnight at 4°C with a polyclonal rabbit anti-Cx43 antibody diluted at 1:400. After three PBS washes, the cells were incubated for 1 h at room temperature with a monoclonal mouse anti-rat HA antibody (Sigma) diluted at 1:500. After three washings with PBS, the cells were incubated for 1 h with FITC-conjugated anti-rabbit IgG (Sigma) diluted at 1:100 and rhodamine-conjugated anti-mouse IgG (Sigma) separately. The cells then were viewed and photographed using a confocal microscope. Green fluorescence indicated positive Cx43 staining, whereas

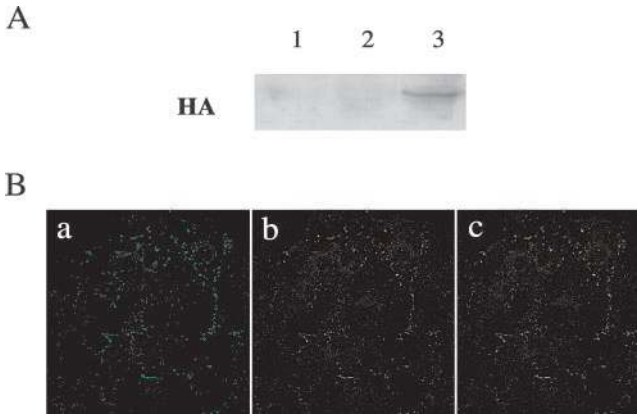

Figure 7. Construction of retroviral vectors and transfection of GMC. (A) Retrovirus-mediated overexpression of Cx43 demonstrated in GMC. Proteins from cells were analyzed using a hemagglutinin (HA) antibody on Western blots. Lane 1, control GMC without transfection; lane 2, GMC transfected with pLNCX2-neo; lane 3, GMC transfected with pLNCX2-Cx43. (B) GMC transfected with pLNCX2-Cx43 were double stained with Cx43 and HA antibodies. Green fluorescence indicates positive Cx43 staining (a), red fluorescence indicates HA expression (b), and yellow color in the merged image indicates co-localization of Cx43 and HA (c). Magnification, ×400.

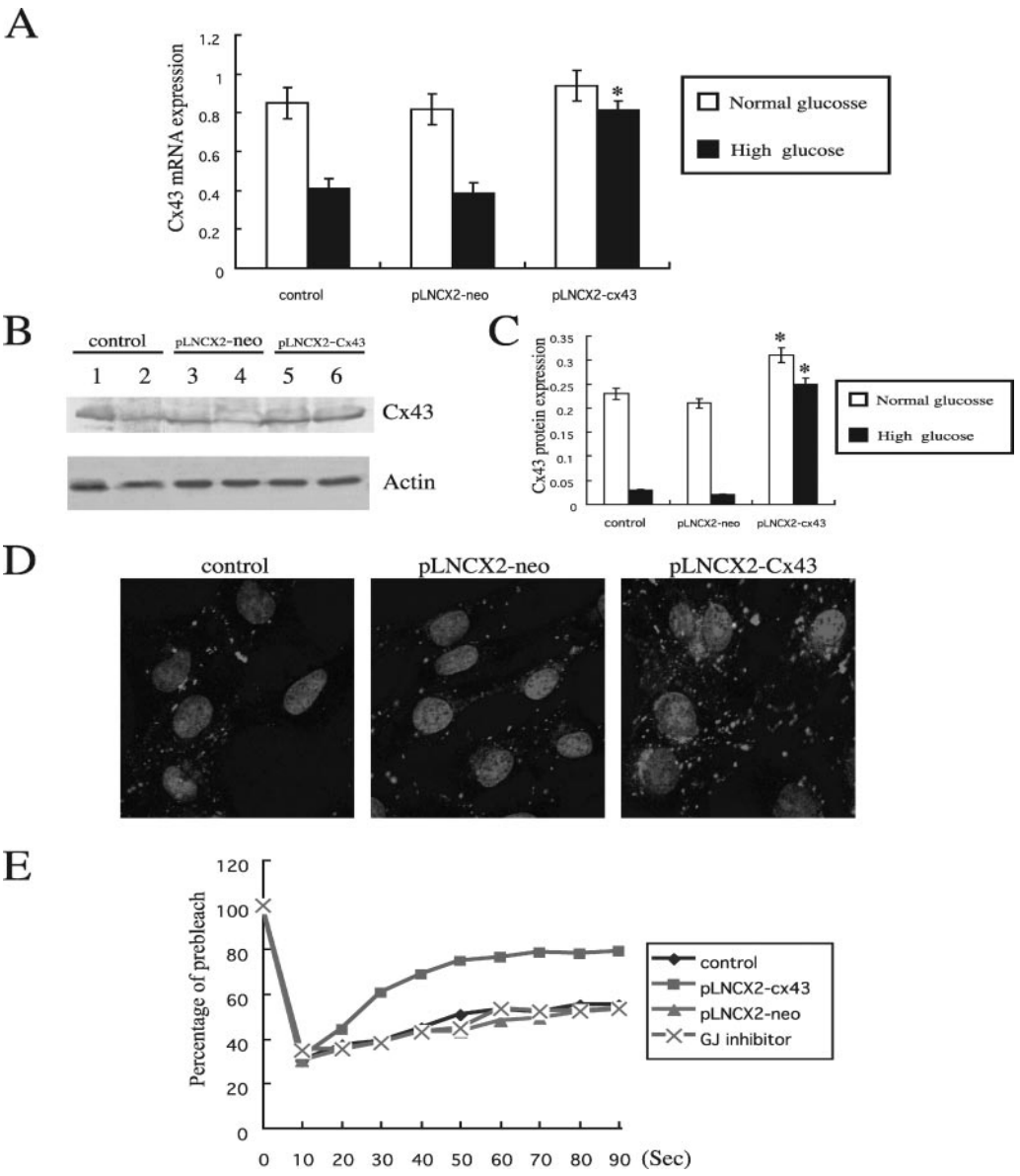

Figure 8. Effect of PLNCX2-Cx43 gene transfection on Cx43 expression and GJIC function in GMC. (A) Cx43 mRNA expression was detected by real-time PCR. GMC transfected with pLNCX2-Cx43 showed significantly higher levels of Cx43 mRNA than control cells or GMC transfected with pLNCX2-neo after 48 h of incubation with high glucose. *$P < 0.05$ *versus* control group ($n = 6$). (B) Western blots of Cx43 protein expression. Lanes 1, 3, and 5, cells were incubated in normal-glucose (5.5 mM) medium for 48 h; lanes 2, 4, and 6, cells were incubated in high-glucose (30 mM) medium for 48 h. (C) Relative Cx43 protein abundance compared with actin. GMC transfected with pLNCX2-Cx43 showed significantly higher levels of Cx43 than cells in the other two groups. *$P < 0.05$ *versus* control group ($n = 6$). (D) Three groups of GMC were incubated in high glucose for 48 h and then immunostained for Cx43 with a monoclonal anti-Cx43 antibody. GMC transfected with pLNCX2-Cx43 showed higher levels of staining of Cx43 at cell–cell contact regions. (E) Fluorescence recovery curve after photobleaching in GMC grown in high-glucose medium for 48 h. Note that GMC transfected with pLNCX2-CX43 showed better GJIC function than control cells or cells transfected by PLNCX2-neo. Pretreatment of GMC with the GJ inhibitor heptanal (0.5 mmol/L) for 30 min blocked the enhancement of GJIC by pLNCX2-Cx43 transfection. Magnification, 600.

red fluorescence indicated HA expression, and orange color indicated co-localization of Cx43 and HA. The efficiency and the specificity of Cx43 overexpression on enhancement of GJIC in GMC were detected by FRAP in the presence or absence of GJ inhibitor heptanal (0.5 mmol/L).

Statistical Analyses

All data analyses were performed with SPSS 10.0 (SPSS Inc., Chicago, IL); data are expressed as mean ± SD. Comparison among groups was conducted with ANOVA. $P < 0.05$ was considered significant.

Results

High Glucose Accelerated Rat GMC Senescence

GMC were cultured for 96 h in normal-glucose (5.5 mM) medium, osmotic control, and high-glucose (30 mM) medium. MTT assays demonstrated that the cellular proliferation capacity of GMC was inhibited by high glucose. The optical density values after 72 h of incubation in high glucose were significantly lower than those in the other two groups ($P < 0.05$; Figure 1). At the same time, the levels of CDK inhibitors $p27^{kip1}$ and $p21^{cip1}$ in GMC were significantly increased under high glucose for 48 h (Figure 2). In addition, the percentage of SA-β-gal stained positive cells in GMC cultured in high glucose for 96 h (70.88 ± 7.19%) was significantly greater than that in normal-glucose medium (30.55 ± 4.86%) or in osmotic control (31.37 ± 5.73; $P < 0.05$; Figure 3), indicating that high glucose induced senescence in GMC.

High Glucose Downregulated Cx43 Expression and GJIC Activity in GMC

The expression of CX43 was detected in GMC cultured in various concentrations of glucose by real-time PCR, Western blot analysis, and immunofluorescence staining. The results showed that the mRNA and protein levels of Cx43 expression of the high-glucose group were significantly lower than those in cells exposed to normal glucose ($P < 0.05$). In addition, immunofluorescence microscopy showed fewer number of Cx43 gap junction plaques at the contact site between adjacent cells grown in high-glucose medium (Figure 4, A through D).

The functional implications of decreased Cx43 expression in GMC exposed to high-glucose medium was evaluated by FRAP analysis (Figure 4E). The degree of intercellular communication was expressed with a fluorescence recovery curve. The results indicated that the recovery rate after photobleaching of cells grown in high glucose (0.60 ± 0.019) was significantly lower than those of the other two groups (0.84 ± 0.023 and 0.82 ± 0.025; $P < 0.05$).

Silencing Cx43 Expression Triggered Hypertrophy and Senescence in GMC

RNA interference has become available and has been proved to be a powerful tool for studying gene function. Short 21- to 23-nucleotide interfering RNA (siRNA) have been used successfully to provide a strong and specific suppression of gene expression in mammalian cells (15,16). In this study, 21-nucleotide interfering RNA (siRNA-Cx43) targeting rat Cx43 sequence was designed and transfected into GMC. To investigate its efficacy, we transfected GMC with either siRNA-Cx43 or irrelevant siRNA-con. After 48 h, the Cx43 expression was assessed by real-time PCR, Western blot, and immunocytochemistry. Our results indicated that Cx43 mRNA were markedly lower in GMC transfected with siRNA-Cx43 than those of control GMC and GMC transfected with siRNA-con (Figure 5). In addition, when siRNA-Cx43 was transfected, gap junction plaques at cell–cell interfaces were less prevalent than those in controls, which coincided with a reduction in total Cx43 expression as revealed by Western blot (Figure 5). Meanwhile, GJIC of GMC was dramatically inhibited by siRNA-Cx43 (Figure 5). All of these data demonstrated that the siRNA-Cx43 was effective in downregulating Cx43 expression and function in GMC.

To examine the consequences of Cx43 silencing on GMC, we evaluated the related cell hypertrophy and senescence parameters mentioned above. It was found that in GMC transfected with siRNA-Cx43, the total protein/cell number ratio (Table 1), the percentages of cells at G1 phase (Table 2), the SA-β-gal positive staining rate, and the expressions of CDK inhibitors $p21^{cip1}$ and $p27^{kip1}$ were significantly higher than those in controls. In addition, the proliferation rate was significantly lower than those of control GMC or siRNA-con GMC (Figure 6). These results suggested that GMC that exhibited reduction in Cx43 expression underwent hypertrophy and premature senescence.

Cx43 Gene Overexpression Prevents GMC Hypertrophy and Premature Senescence Induced by High Glucose

Because it was difficult to transfect genes efficiently into GMC using plasmids, we created a retroviral vector pLNCX2-Cx43, which drives HA-tagged Cx43. This construct was confirmed with *Bgl II* and SalI digestion. The retrovirus that was produced by packaging PT-67 cells was collected and infected GMC effectively, as demonstrated by Western blot and double immunofluorescence staining of Cx43 and HA tag (Figure 7).

GMC transfected with pLNCX2-Cx43 showed not only higher levels of Cx43 mRNA and protein but also better GJIC function in high glucose for 48 h (Figure 8) than in control cells and cells transfected by pLNCX2-neo ($P < 0.05$). Pretreatment of GMC with heptanal (0.1 mM) blocked GJIC enhancement by Cx43 overexpression, which demonstrated specific activation of Cx43. Moreover, it was found that cell hypertrophy and the senescence-related phenotypes of GMC promoted by high glucose were ameliorated in GMC that expressed exogenous Cx43 (Table 3, Figure 9). In GMC transfected with pLNCX2-Cx43 and cultured in high glucose, the percentage of cells at G1 phase (64.23 ± 2.35%) was significantly lower than that of control cells

Table 3. Cx43 gene overexpression prevents GMC hypertrophy induced by high glucose[a]

	Control	pLNCX2-neo	pLNCX2-Cx43
Protein/cell number ratio	30.78 ± 4.31	31.59 ± 3.18	25.72 ± 2.03[b]

[a]GMC that were transfected with pLNCX2-Cx43 and pLNCX2-neo were incubated in high glucose for 72 h. The total protein/cell number ratio was expressed as $\mu g/10^5$ cells. Values are presented as means ± SD ($n = 6$); comparison among groups was conducted by ANOVA.

[b]$P < 0.05$ *versus* control group.

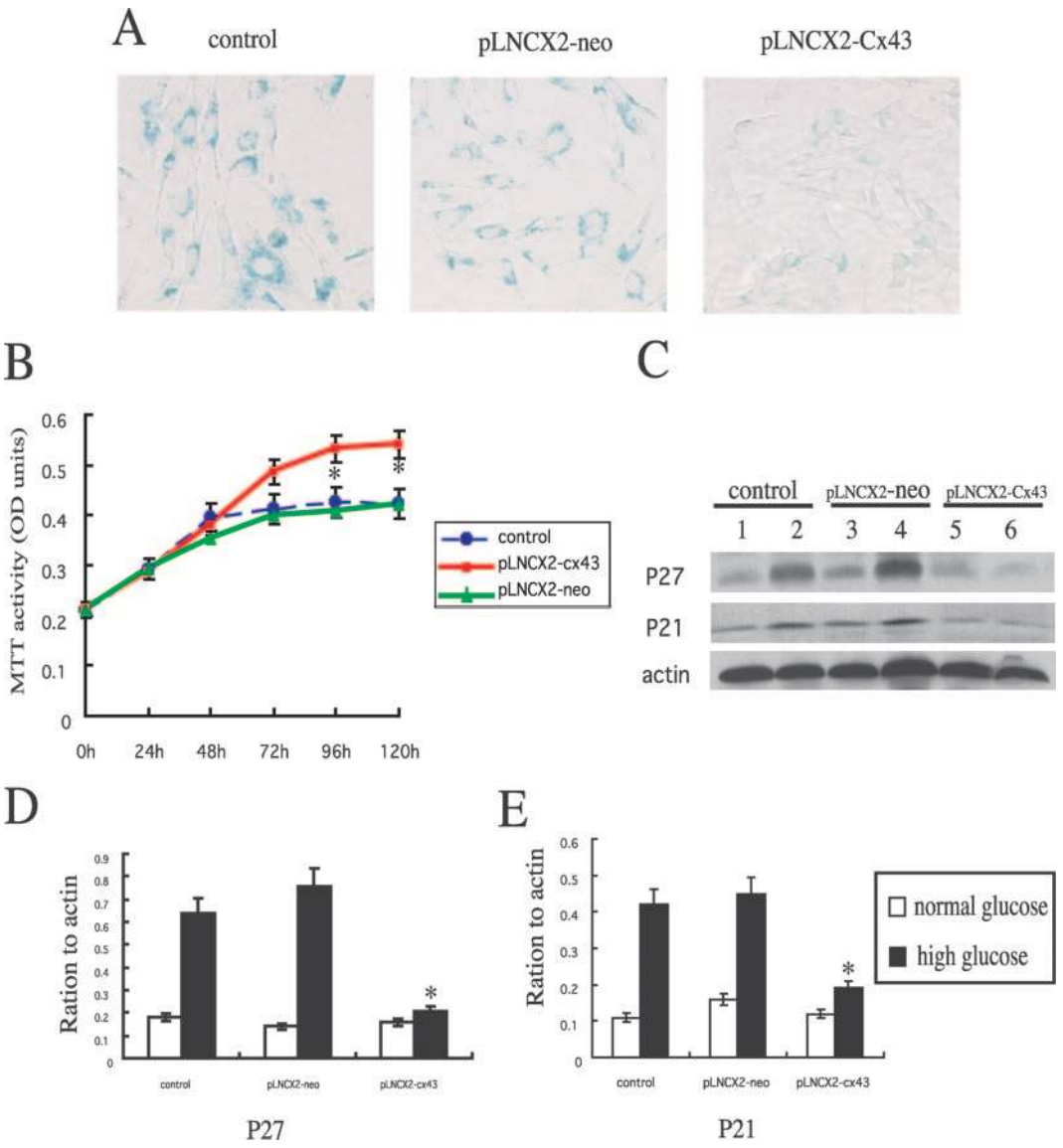

Figure 9. Senescence-related phenotypes of GMC transfected with pLNCX2-Cx43. (A) Effect of Cx43 gene transfection on SA-β-gal staining in GMC incubated in high glucose. The percentage of SA-β-gal–positive cells transfected with pLNCX2-Cx43 was lower than that of control or cells transfected with pLNCX2-neo. (B) Proliferation of GMC under high glucose. Note that cell proliferation of cells transfected with pLNCX2-Cx43 was higher than that of controls or cells transfected with pLNCX2-neo. *$P < 0.05$ *versus* control group ($n = 6$). (C) Western blot demonstrating expression of $p27^{kip1}$ and $p21^{cip1}$ in cells transfected with pLNCX2-Cx43 compared with controls. Cells were incubated in normal glucose (5.5 mM) for 48 h (lanes 1, 3, and 5) or in high glucose for 48 h (lanes 2, 4, and 6). (D) Relative $p27^{kip1}$ and $p21^{cip1}$ protein abundances normalized to actin. *$P < 0.05$ *versus* control group cultured in high glucose ($n = 6$). Magnification, ×200.

(75.95 ± 5.09%) or that of cells transfected with pLNCX2-neo (72.09 ± 1.60%; Table 4). Cx43 gene transfection also decreased $p21^{cip1}$ and $p27^{kip1}$ protein levels (Figure 9) in GMC cultured in high glucose.

Discussion

In this study, we examined senescence-related phenotypes and gap junction alterations of GMC exposed to high glucose concentrations. Cx43 silencing and overexpressing techniques were used to demonstrate the potential function of Cx43 in this pathologic condition. Our results address the protective role of Cx43 in regulating GMC growth and phenotype.

It is known that most types of primary normal cells do not proliferate indefinitely. After a period of rapid proliferation, cell division rates decrease and ultimately cease; the cells then enter a state of senescence that is characterized by an irreversible G_1 growth arrest and functional and morphologic changes (4,17). Senescence of cells also can occur rapidly in response to various physiologic stresses, such as high glucose, oxidative stress (18), DNA-damaging agents, and other metabolic perturbations.

In this study, we detected β-gal activity of GMC cultured in various doses of glucose, as one of many hallmark measures of cell replicative senescence or physiologic aging (19). The results

Table 4. Cx43 gene overexpression prevents the cell-cycle arrest of GMC induced by high glucose[a]

	Control	pLNCX2-Cx43	pLNCX2-neo
G1 phase (%)	75.95 ± 5.09	64.23 ± 2.35[b]	72.09 ± 1.60
S phase (%)	14.51 ± 1.24	32.52 ± 2.02[b]	21.87 ± 2.91

[a]GMC that were transfected with pLNCX2-Cx43 and pLNCX2-neo were incubated in high glucose for 72 h and then stained with propidium iodide and analyzed by flow cytometry. Values are means ± SD ($n = 6$); comparison among groups was conducted with ANOVA.
[b]$P < 0.05$ *versus* control group.

indicated that the percentage of SA-β-gal positive stained cells cultured in high-glucose medium was significantly greater than that of cells in normal-glucose medium or in osmotic control. In addition, GMC cultured in high glucose were characterized by an irreversible G_1 growth arrest and also associated with the upregulation of cell-cycle inhibitors $p21^{cip1}$ and $p27^{kip1}$, which were similar to the results of some other studies (2,3) in which these parameters were used to measure cell senescence. Our results demonstrated that high glucose induced senescence in GMC.

The mechanisms of cell senescence are not clear; growing evidence has shown that Cx43 and GJIC might be involved in this process. Gap junctions are intercellular channels that permit the passage of small molecules such as small metabolites, ions, and second messengers. GJIC has an important role in a variety of cellular processes, including homeostasis, morphogenesis, cell differentiation, and growth control (20,21). Statuto *et al.* (22) reported a progressive decrease of the expression of Cx43 and GJIC in replicative senescence of cultured HEL-299 fibroblasts and termed Cx43 as a biomarker of cell senescence. It also has been shown that the expression and function of Cx43 in astrocytic cells and aortic endothelium were age related, suggesting that Cx43 and GJIC may play a role in the process of cell aging (23–26).

Studies already have shown that Cx43 is a major connexin in GMC. There is a high density of Cx43 expression in GMC (27,28); however, little is known about its exact functions. It has been suggested that Cx43 may have a role in connecting GMC into a functional syncytium (29–31). Gap junction–mediated cell–cell communication may play a role in the stringent growth control of GMC. There are few data, however, concerning functional regulation of Cx43 and GJIC in GMC under pathologic circumstances.

This is the first report to explore the relationship between Cx43 function and senescence of GMC in high glucose. As the first step, we evaluated whether high glucose affected GMC connexin expression and GJIC activity. The results showed that Cx43 expression and the number of Cx43 gap junctions were significantly downregulated by high glucose, which was consistent with some previous results (8,9,11,32). Cx43 family members degrade rapidly, with half-lives of only 1.5 to 5 h (21), suggesting that the reduction of Cx43 expression could be attributed to decreased transcription and translation of Cx43 gene in high glucose. As a result, the reduced GJIC activity in GMC that are exposed to high glucose could impair the transport of small molecules, such as calcium or cAMP, that are necessary for cell proliferation and maintenance of cellular homeostasis.

To explore the exact role of Cx43 in GMC senescence that is induced by high glucose, we used Cx43 gene knockdown and overexpression successfully to silence or enhance Cx43 expression. The results have shown that GMC infected with siRNA-Cx43 displayed the phenotypes of senescence, as demonstrated by SA-β-gal staining and increased $p27^{kip1}$ and $p21^{cip1}$. In contrast, GMC transfected with the retrovirus pLNCX2-Cx43 displayed both higher levels of Cx43 expression and improved senescence-related phenotypes in high glucose. It therefore is reasonable to suggest that there may be an association between decreased Cx43 expression and cell senescence in high glucose. The loss of Cx43 may result in unregulated cell proliferation and contribute, at least in part, to the cell senescence at high glucose.

To determine the mechanism by which Cx43 regulates GMC growth and senescence, we examined potential molecules that are regulated by Cx43. It is known that cell proliferation and senescence are regulated at the level of the cell cycle by cell-cycle proteins, including CDK. In contrast, CDK inhibitors inactivate CDK and cause cell-cycle arrest. There is a growing body of literature showing that CDK inhibitors $p21^{cip1}$ and $p27^{kip1}$ may be critical regulators of GMC hypertrophy (33) and cell senescence (4,34). Zheng *et al.* (5) found that mesangial cells isolated from kidneys of postmenopausal mice were enlarged and had elevated amounts of $p27^{kip1}$ protein expression as assessed by immunochemistry. Other studies (35–37) also showed that $p21^{cip1}$ and $p27^{kip1}$ were required for retinoblastoma protein–mediated senescence, demonstrating not only that $p21^{cip1}$ and $p27^{kip1}$ gene transfer could promote cell senescence but also that antisense $p21^{cip1}$ and $p27^{kip1}$ had some effects on retarding the progress of cell hypertrophy or senescence. Our results showed that Cx43 knockdown significantly increased $p21^{cip1}$ and $p27^{kip1}$ expression in GMC, whereas Cx43 gene overexpression decreased $p21^{cip1}$ and $p27^{kip1}$ protein levels in GMC cultured in high glucose, indicating that Cx43 could control cell proliferation and senescence progression through cell-cycle regulation.

Conclusion

Our data have demonstrated for the first time that hyperglycemia-mediated reduction of Cx43 expression and GJIC activity is involved in the development of cell hypertrophy and senescence in GMC. This might be a potential target for treating diabetic nephropathy.

Acknowledgments

This work was supported by grants from the Creative Research Group Fund of the National Foundation Committee of Natural Science of China (30121005), the National Natural Sciences Foundation of China (30370655 and 30300161), and the Main State Basic Research Development Program of China.

References

1. Wolf G: Cell cycle regulation in diabetic nephropathy. *Kidney Int* 77[Suppl]: S59–S66, 2000
2. Wolf G, Reinking R, Zahner G, Stahl RA, Shankland SJ: Erk 1,2 phosphorylates p27(Kip1): Functional evidence for a role in high glucose-induced hypertrophy of mesangial cells. *Diabetologia* 46: 1090–1099, 2003
3. Al-Douahji M, Brugarolas J, Brown PA, Stehman-Breen CO, Alpers CE, Shankland SJ: The cyclin kinase inhibitor p21WAF1/CIP1 is required for glomerular hypertrophy in experimental diabetic nephropathy. *Kidney Int* 56: 1691–1699, 1999
4. Ben-Porath I, Weinberg RA: When cells get stressed: An integrative view of cellular senescence. *J Clin Invest* 113: 8–13, 2004
5. Zheng F, Plati AR, Banerjee A, Elliot S, Striker LJ, Striker GE: The molecular basis of age-related kidney disease. *Sci Aging Knowledge Environ* 29: 20–28, 2003
6. Blazer S, Khankin E, Segev Y, Ofir R, Yalon-Hacohen M, Kra-Oz Z, Gottfried Y, Larisch S, Skorecki KL: High glucose-induced replicative senescence: Point of no return and effect of telomerase. *Biochem Biophys Res Commun* 296: 93–101, 2002
7. Morocutti A, Earle KA, Sethi M, Piras G, Pal K, Richards D, Rodemann P, Viberti G: Premature senescence of skin fibroblasts from insulin-dependent diabetic patients with kidney disease. *Kidney Int* 50: 250–256, 1996
8. Fernandes R, Giro H, Pereira P: High glucose down-regulates intercellular communication in retinal endothelial cells by enhancing degradation of connexin 43 by a proteasome-dependent mechanism. *J Biol Chem* 279: 27219–27224, 2004
9. Kuroki T, Inoguchi T, Umeda F, Ueda F, Nawata H: High glucose induces alteration of gap junction permeability and phosphorylation of connexin-43 in cultured aortic smooth muscle cells. *Diabetes* 47: 931–936, 1998
10. Li AF, Sato T, Haimovici R, Okamoto T, Roy S: High glucose alters connexin 43 expression and gap junction intercellular communication activity in retinal pericytes. *Invest Ophthalmol Vis Sci* 44: 5376–5382, 2003
11. Sato T, Haimovici R, Kao R, Li AF, Roy S: Downregulation of connexin 43 expression by high glucose reduces gap junction activity in microvascular endothelial cells. *Diabetes* 51: 1565–1571, 2002
12. Li Z, Chen X, Xie Y, Shi S, Feng Z, Fu B, Zhang X, Cai G, Wu C, Wu D, Gu Y: Expression and significance of integrin-linked kinase in cultured cells, normal tissue, and diseased tissue of aging rat kidneys. *J Gerontol A Biol Sci Med Sci* 59: 984–996, 2004
13. Nagai K, Matsubara T, Mima A, Sumi E, Kanamori H, Iehara N, Fukatsu A, Yanagita M, Nakano T, Ishimoto Y, Kita T, Doi T, Arai H: Gas6 induces Akt/mTOR-mediated mesangial hypertrophy in diabetic nephropathy. *Kidney Int* 68: 552–561, 2005
14. Storrie B, Pepperkok R, Stelzer EH, Kreis TE: The intracellular mobility of a viral membrane glycoprotein measured by confocal microscope fluorescence recovery after photobleaching. *J Cell Sci* 107: 1309–1319, 1994
15. Elbashir SM, Harborth J, Lendeckel W, Yalcin A, Weber K, Tuschl T: Duplexes of 21-nucleotide RNAs mediate RNA interference in cultured mammalian cells. *Nature* 411: 494–498, 2001
16. Wu D, Chen X, Guo D, Hong Q, Fu B, Ding R, Yu L, Hou K, Feng Z, Zhang X, Wang J: Knockdown of fibronectin induces mitochondria-dependent apoptosis in rat mesangial cells. *J Am Soc Nephrol* 16: 646–657, 2005
17. Sharpless NE, DePinho RA: Telomeres, stem cells, senescence, and cancer. *J Clin Invest* 113: 160–168, 2004
18. Ho HY, Cheng ML, Lu FJ, Chou YH, Stern A, Liang CM, Chiu DT: Enhanced oxidative stress and accelerated cellular senescence in glucose-6-phosphate dehydrogenase (G6PD)-deficient human fibroblasts. *Free Radic Biol Med* 29: 156–169, 2000
19. Dimri GP, Lee X, Basile G, Acosta M, Scott G, Roskelley C, Medrano EE, Linskens M, Rubelj I, Pereira-Smith O: A biomarker that identifies senescent human cells in culture and in aging skin in vivo. *Proc Natl Acad Sci U S A* 92: 9363–9367, 1995
20. Goodenough DA, Paul DL: Beyond the gap: Functions of unpaired connexon channels. *Nat Rev Mol Cell Biol* 4: 285–294, 2003
21. Saez JC, Berthoud VM, Branes MC, Martinez AD, Beyer EC: Plasma membrane channels formed by connexins: Their regulation and functions. *Physiol Rev* 83: 1359–1400, 2003
22. Statuto M, Bianchi C, Perego R, Del Monte U: Drop of connexin 43 in replicative senescence of human fibroblasts HEL-299 as a possible biomarker of senescence. *Exp Gerontol* 37: 1113–1120, 2002
23. Jones SA, Lancaster MK, Boyett MR: Ageing-related changes of connexins and conduction within the sinoatrial node. *J Physiol* 560: 429–437, 2004
24. Yeh HI, Chang HM, Lu WW, Lee YN, Ko YS, Severs NJ, Tsai CH: Age-related alteration of gap junction distribution and connexin expression in rat aortic endothelium. *J Histochem Cytochem* 48: 1377–1389, 2000
25. Cotrina ML, Gao Q, Lin JH, Nedergaard M: Expression and function of astrocytic gap junctions in aging. *Brain Res* 901: 55–61, 2001
26. Dilley TK, Bowden GT, Chen QM: Novel mechanisms of sublethal oxidant toxicity: Induction of premature senescence in human fibroblasts confers tumor promoter activity. *Exp Cell Res* 290: 38–48, 2003
27. Guo R, Liu L, Barajas L: RT-PCR study of the distribution of connexin 43 mRNA in the glomerulus and renal tubular segments. *Am J Physiol* 275: R439–R447, 1998
28. Hillis GS, Duthie LA, Mlynski R, McKay NG, Mistry S, MacLeod AM, Simpson JG, Haites NE: The expression of connexin 43 in human kidney and cultured renal cells. *Nephron* 75: 458–463, 1997
29. Yao J, Morioka T, Oite T: PDGF regulates gap junction communication and connexin43 phosphorylation by PI 3-kinase in mesangial cells. *Kidney Int* 57: 1915–1926, 2000
30. Yao J, Suwa M, Li B, Kawamura K, Morioka T, Oite T: ATP-dependent mechanism for coordination of intercellu-

lar Ca2+ signaling and renin secretion in rat juxtaglomerular cells. *Circ Res* 93: 338–345, 2003
31. Ryan MJ, Liu B, Herbowy MT, Gross KW, Hajduczok G: Intercellular communication between renin expressing As4.1 cells, endothelial cells and smooth muscle cells. *Life Sci* 72: 1289–1301, 2003
32. Inoguchi T, Yu HY, Imamura M, Kakimoto M, Kuroki T, Maruyama T, Nawata H: Altered gap junction activity in cardiovascular tissues of diabetes. *Med Electron Microsc* 34: 86–91, 2001
33. Wolf G, Schroeder R, Zahner G, Stahl RA, Shankland SJ: High glucose-induced hypertrophy of mesangial cells requires p27(Kip1), an inhibitor of cyclin-dependent kinases. *Am J Pathol* 158: 1091–1100, 2001
34. Chkhotua AB, Gabusi E, Altimari A, D'Errico A, Yakubovich M, Vienken J, Stefoni S, Chieco P, Yussim A, Grigioni WF: Increased expression of p16(INK4a) and p27(Kip1) cyclin-dependent kinase inhibitor genes in aging human kidney and chronic allograft nephropathy. *Am J Kidney Dis* 41: 1303–1313, 2003
35. Alexander K, Hinds PW: Requirement for p27(KIP1) in retinoblastoma protein-mediated senescence. *Mol Cell Biol* 21: 3616–3631, 2001
36. Jirawatnotai S, Moons DS, Stocco CO, Franks R, Hales DB, Gibori G, Kiyokawa H: The cyclin-dependent kinase inhibitors p27Kip1 and p21Cip1 cooperate to restrict proliferative life span in differentiating ovarian cells. *J Biol Chem* 278: 17021–17027, 2003
37. Awazu M, Omori S, Ishikura K, Hida M, Fujita H: The lack of cyclin kinase inhibitor p27(Kip1) ameliorates progression of diabetic nephropathy. *J Am Soc Nephrol* 14: 699–708, 2003